INTERFACE

rsif.royalsocietypublishing.org

Research

**Cite this article:** Font-Muñoz JS, Jordi A, Tuval I, Arrieta J, Anglès S, Basterretxea G. 2017 Advection by ocean currents modifies phytoplankton size structure. *J. R. Soc. Interface* **14**: 20170046.
http://dx.doi.org/10.1098/rsif.2017.0046

Received: 23 January 2017
Accepted: 6 April 2017

**Subject Category:**
Life Sciences–Earth Science interface

**Subject Areas:**
environmental science

**Keywords:**
plankton, coastal circulation, cell size distribution, preferential concentration, inertial properties, Mediterranean Sea

**Author for correspondence:**
Joan S. Font-Muñoz
e-mail: jfont@imedea.uib-csic.es

Electronic supplementary material is available online at https://dx.doi.org/10.6084/m9.figshare.c.3744341.

THE ROYAL SOCIETY PUBLISHING

# Advection by ocean currents modifies phytoplankton size structure

Joan S. Font-Muñoz[1], Antoni Jordi[2], Idan Tuval[1], Jorge Arrieta[1], Sílvia Anglès[1] and Gotzon Basterretxea[1]

[1]Institut Mediterrani d'Estudis Avançats, IMEDEA (UIB-CSIC), Esporles, Illes Balears, Spain
[2]Davidson Laboratory, Stevens Institute of Technology, Hoboken, NJ, USA

JSF-M, 0000-0001-6964-8866; AJ, 0000-0003-2637-8389; IT, 0000-0002-6629-0851; JA, 0000-0003-1260-6168; SA, 0000-0003-0529-7504; GB, 0000-0001-7466-1360

Advection by ocean currents modifies phytoplankton size structure at small scales (1–10 cm) by aggregating cells in different regions of the flow depending on their size. This effect is caused by the inertia of the cells relative to the displaced fluid. It is considered that, at larger scales (greater than or equal to 1 km), biological processes regulate the heterogeneity in size structure. Here, we provide observational evidence of heterogeneity in phytoplankton size structure driven by ocean currents at relatively large scales (1–10 km). Our results reveal changes in the phytoplankton size distribution associated with the coastal circulation patterns. A numerical model that incorporates the inertial properties of phytoplankton confirms the role of advection on the distribution of phytoplankton according to their size except in areas with enhanced nutrient inputs where phytoplankton dynamics is ruled by other processes. The observed preferential concentration mechanism has important ecological consequences that range from the phytoplankton level to the whole ecosystem.

## 1. Introduction

Phytoplankton size structure plays a fundamental role in marine ecosystems. It responds to environmental conditions while controlling the biogeochemical cycling of many elements, through carbon fixation and phosphorous exportation [1–3]. Small cells (less than 2 µm) account for up to 80% of the bulk of phytoplankton biomass in open-ocean oligotrophic waters [4]. As a result of their small size, sedimentation is slow and most elements are recycled within the photic layer through complex microbial food webs [5]. Therefore, small phytoplankton have limited potential to regulate atmospheric carbon dioxide levels [6]. By contrast, large cells (greater than 20 µm) dominate in nutrient-rich productive waters such as river-influenced zones or upwelling areas [7]. Owing to their enhanced sedimentation rate, a larger fraction of primary production is exported from the euphotic zone towards the ocean interior, thus contributing to carbon dioxide sequestration [8].

Both biological and physical processes may contribute to modify the patterns of phytoplankton size [9]. On one hand, it is generally accepted that biological processes drive heterogeneity at large spatial scales (greater than or equal to 1 km) [10]. Phytoplankton cell size influences growth and metabolic rates, access to and assimilation of resources, and determines cell susceptibility to grazing [1,11]. For example, nutrient requirements to sustain phytoplankton vital rates are roughly proportional to the inverse of cell size [12,13]. Therefore, larger cells are at a disadvantage compared with smaller cells at low nutrient concentrations such as those found in oligotrophic waters [14,15]. Likewise, increasing cell size is a successful escape strategy to avoid certain grazer types [16].

On the other hand, advection and mixing by ocean currents are among the primary physical forcing experienced by any marine organism, especially by phytoplankton. Traditionally, the effect of small-scale turbulence on phytoplankton transport was thought to act as a means for creating homogeneous distributions because phytoplankton cells were assumed as infinitesimal passive particles [9]. However, phytoplankton cells have a finite size and different inertial

properties with respect to the surrounding fluid. Therefore, they do not acquire the fluid velocity instantly. This effect is not necessarily negligible and is taken into account both in natural and industrial applications [17–19]. In fact, recent theoretical studies suggest that advection by ocean turbulence aggregates cells in different regions of the flow depending on their size and/or density due to their inertia [20,21]. Smaller and lighter cells are attracted by the regions of turbulence with high vorticity and remain accumulated inside the vortical structures of the flow. By contrast, larger and heavier cells tend to preferentially concentrate in regions of low fluid vorticity [22,23]. This particle sorting mechanism is also observed in neutral buoyancy particles in three-dimensional flows [24]. However, those studies are based on laboratory experiments at microscales and/or on numerical simulations. To our knowledge, preferential concentration as a function of cell size has not yet been observed in the ocean at large scales (greater than or equal to 1 km).

In this study, we analyse the role of advection on the spatial distribution of phytoplankton using field measurements and numerical simulations that consider the inertial properties of the cells. The aim is to evaluate whether advection alone is able to modify the patterns of phytoplankton size at scales larger than 1 km. The study was carried out in the inner part of Palma Bay (Mallorca Island, Mediterranean Sea, see figure 1). Phytoplankton biomass is generally low around Mallorca due to the prevailing oligotrophic conditions in the Mediterranean Sea and to the absence of rivers in the island [25,26]. However, groundwater discharges from the nitrate rich aquifers can locally enhance primary production around Mallorca Island [27,28]. Furthermore, phytoplankton biomass in Palma Bay remarkably increases after intense rainfall events due to a few torrents that flow into the bay [29]. In addition, ocean circulation around Mallorca Island is mainly driven by two wind-forced mechanisms: remotely generated island trapped waves and a local wind-induced response [30–32]. We combine field data on current velocity and particle size measurements with numerical simulations to verify the role of advection on the distribution of phytoplankton according to their size.

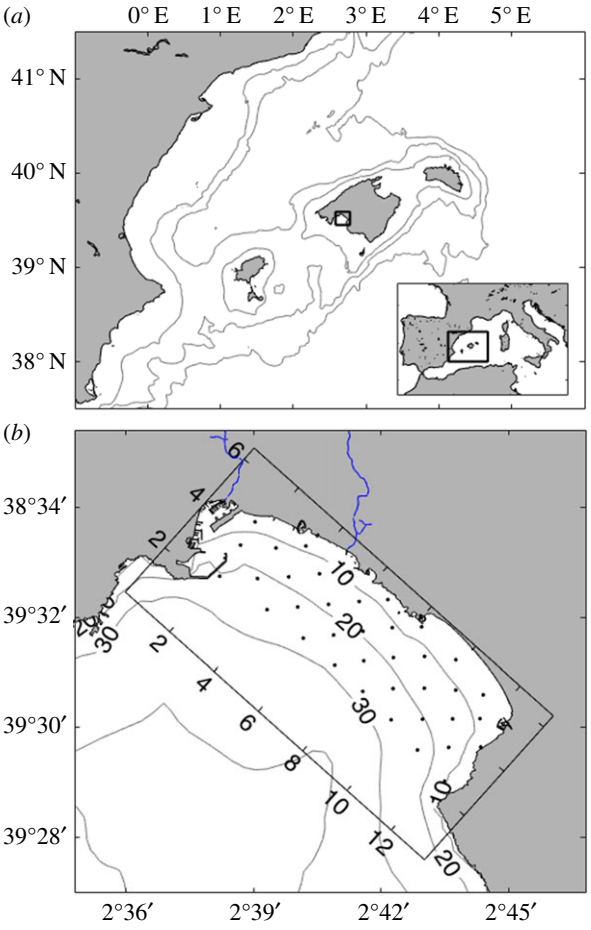


**Figure 1.** Study area and sampling stations. (*a*) Map showing the location of the Balearic Islands (bottom right), the location of Palma Bay (black square) and bathymetry (m, grey lines) around the Balearic Islands. (*b*) Bathymetry (m, grey lines) in the inner part of Palma Bay showing the position of the sampling stations (black dots). The units of the rotated axes in (*b*) are km. (Online version in colour.)

## 2. Material and methods

Measurements of particle size structure, chlorophyll, nutrient concentrations and ocean currents were obtained in two surveys carried out in the inner part of Palma Bay on 16 June and 25 September 2009. To determine the phytoplankton size structure, simultaneous measures of particle distribution in 32 size classes (logarithmically spaced from 2.5 to 500 µm) and chlorophyll concentration were continuously registered from the surface to the sea bottom in a grid of 37 stations (figure 1) using a laser *in situ* scattering and transmissometry instrument (LISST-100X, Sequoia Scientific) and a Seabird-25 CTD equipped with a Cyclops-7 fluorometer (Turner Designs), respectively. The fluorometer was calibrated with a surface sample obtained at each station, filtered through a Whatman GF/F filter and analysed in the laboratory using a linear least-squares fit ($r^2 = 0.94$). Throughout this study, we use chlorophyll as a proxy of phytoplankton biomass. Phytoplankton size structure and abundance were separated from particle size distribution using a canonical correlation analysis (CCA) along with the chlorophyll concentration [29]. Nutrient concentrations of dissolved inorganic nitrogen ($DIN = NO_3 + NO_2 + NH_4$) were measured with an Alliance autoanalyser following Grasshoff *et al.* [33] in the same grid of 37 stations. Ocean horizontal currents were recorded with a 1200 kHz RDI Workhorse Sentinel acoustic Doppler current profiler (ADCP) mounted on an Endeco/YSI 703 V-Fin [31]. The V-Fin was towed from the stern of the vessel at a depth of 3 m to avoid ship wake interference with the ADCP. The speed of the vessel was about 3.5 m $s^{-1}$. Currents were recorded at 1 m depth bins from 4 to 16 m every 1 s and then averaged at 1 min ensembles. Phytoplankton size structure, nutrient concentrations and ocean currents were interpolated to obtain regular horizontal fields on a horizontal grid of 300 × 300 m using optimal statistical interpolation [34] with a cut-off length scale of 2000 m to eliminate the smaller scales that cannot be resolved by sampling. Only surface data (4 m) are shown here, although results at deeper levels were very similar.

We used a model to simulate the process of preferential accumulation of certain size particles within specific regions of the current field. The model only takes into account the physical interaction between inertial passive particles and the measured near-surface (two-dimensional) ocean currents. We considered phytoplankton cells as passive particles because our interest was to model the effect of advection considering the inertial properties of phytoplankton cells. The model does not take into account any other physical or biological process. Advection of small but inertial spherical particles is well described by the Maxey–Riley equations [35] and it is determined by two non-dimensional parameters: the particle's Stokes number $St = 2a^2\omega_0/(9\nu R)$ and their mass ratio $R = \rho_F/(\rho_0 + \rho_F/2)$, where $a$ is the radius of the spherical particle, $\rho_0$ and $\rho_F$ are, respectively,

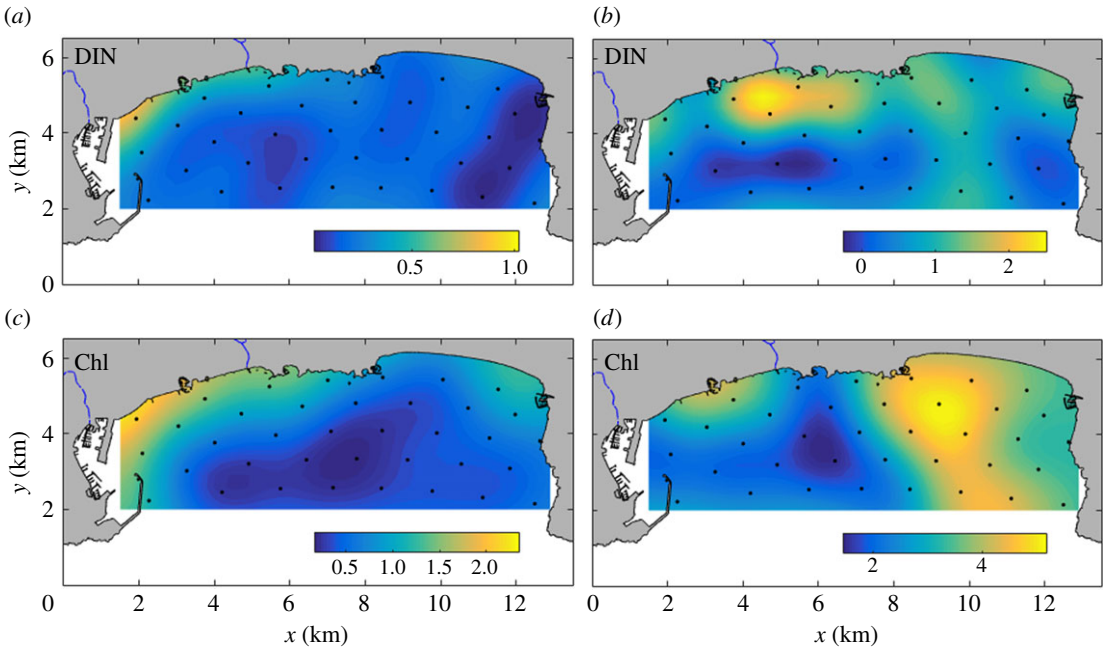


**Figure 2.** Spatial distribution of DIN and chlorophyll. Near-surface distributions of (*a*) DIN (μM) for the June survey, (*b*) DIN (μM) for the September survey, (*c*) chlorophyll (mg $m^{-3}$) for the June survey and (*d*) chlorophyll (mg $m^{-3}$) for the September survey. Black dots indicate the sampling stations. Blue lines over land indicate Sa Riera and Gros Torrents. (Online version in colour.)

the density of the particle and of the surrounding fluid, $\nu$ its kinematic viscosity and $\omega_0$ its maximum vorticity (obtained computing the curl of the measured velocity field, $\omega = \nabla \times u$). However, for phytoplankton cells in the ocean, the range of Stokes number is $St \ll 1$ and we can accurately use the asymptotic limit of this equation [36]:

$$\frac{d^2\mathbf{x}_p}{dt^2} = \mathbf{u}_b + St\left(\frac{3R}{2} - 1\right)\frac{D\mathbf{u}_b}{Dt}. \tag{2.1}$$

We run our Lagrangian simulations by integrating equation (2.1) with a fourth-order Runge–Kutta scheme. Initial conditions for the position and the velocity of the particles were chosen to minimize propagation of errors in the model coming from interpolation errors from the field measurements. The Lagrangian trajectories were integrated with absorbing boundary conditions and within the same domain used to define the horizontal regular grid for the field data (see figure 1*b*). A simple forward extrapolation scheme was used to decide whether a particular trajectory escaped the domain at a given time step after which, if that was the case, the integration was halted. Each trajectory was integrated for either five times the characteristic timescale of the measured flow field (i.e. $T = 5/\omega_0$) or until it leaves the spatial domain through the open (southern) boundary. Spatial binarization was used to assign particle position to nearest-neighbour coarse-grained spatial boxes which allow us to construct a matrix for the stationary distribution of particles' relative abundance. Further details on the numerical model and its performance are provided in the electronic supplementary material.

In order to assess the effect of currents on the distribution of phytoplankton, we fixed $R$ to 0.4 [37] and focus instead on the effect of particle sizes. We swept $a$ in the range 2.5–500 μm (equivalent to the 32 size classes measured *in situ*) and built the stationary distribution for each value. For both measured—obtained from LISST-100X measurements using CCA analysis—and modelled phytoplankton size distributions, we computed the areas of higher/lower particle accumulation as the probability matrix for positive and negative size anomalies, i.e. the overabundance of small (or large) particles. Positive (or negative) values indicate increased (decreased) concentration of small (large) cells. In the model, the observed behaviour is almost independent of the exact choice of the size threshold used to define the separation between small and large particles (variations less than 10% for the separation in the 20–100 μm range). In the measured data, we used the standardized abundances of the two dominant size classes (see below).

## 3. Results

Meteorological conditions during summer in Mallorca are characterized by warm temperatures, low rainfall and weak winds dominated by sea breeze [38]. These were the conditions during the June survey, although a relatively strong wind event (greater than 7 m $s^{-1}$) was registered 3 days before (see electronic supplementary material, figure S3). By contrast, heavy rains (greater than 45 mm $d^{-1}$) occurred on the days prior to the September survey, resulting in significant freshwater discharges through Sa Riera and Gros Torrents (greater than 0.7 $m^3$ $s^{-1}$). Wind forcing was very weak (less than 2 m $s^{-1}$) during the September survey.

Freshwater discharges largely determined DIN availability during both surveys (figure 2). The highest DIN concentrations (greater than 0.9 μM) during the June survey were associated with Palma Harbour, which is the major commercial port in Mallorca and it is subjected to anthropogenic discharges. Chlorophyll maximum (greater than 2 mg $m^{-3}$) was near Palma Harbour in agreement with the DIN inputs, although a secondary maximum (greater than 1.2 mg $m^{-3}$) was present in the eastern side of the bay. In this area, groundwater discharges usually enhance phytoplankton biomass [39]. During the September survey, DIN concentrations were strongly regulated by the freshwater discharges, especially at Gros Torrent. In fact, DIN concentrations in the bay were inversely correlated with salinity ($r = 0.6$, $p < 0.01$, not shown) measured at the same stations. As a result of the increased DIN availability, high chlorophyll concentrations (greater than 3 mg $m^{-3}$) were

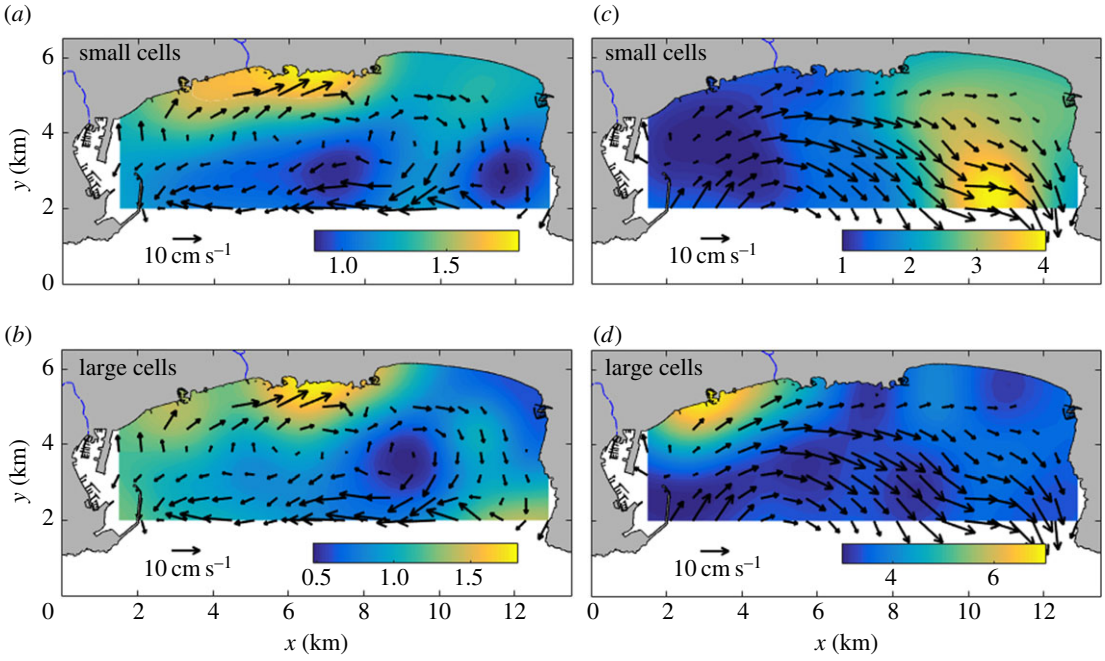


**Figure 3.** Spatial distribution of small and large phytoplankton corresponding to 11.91 ± 3.24 and 30.23 ± 5.58 µm in June and 12.28 ± 3.65 and 30.88 ± 6.29 µm in September, and currents. Near-surface distributions of (*a*) small and (*b*) large phytoplankton size range (colours, $10^5$ and $10^4$ cells $l^{-1}$, respectively) for the June survey, and (*c*) small and (*d*) large phytoplankton size range (colours, $10^5$ and $10^4$ cells $l^{-1}$, respectively) for the September survey. Vectors indicate near-surface ocean currents (cm $s^{-1}$) for the corresponding survey. Blue lines over land indicate Sa Riera and Gros Torrents. (Online version in colour.)

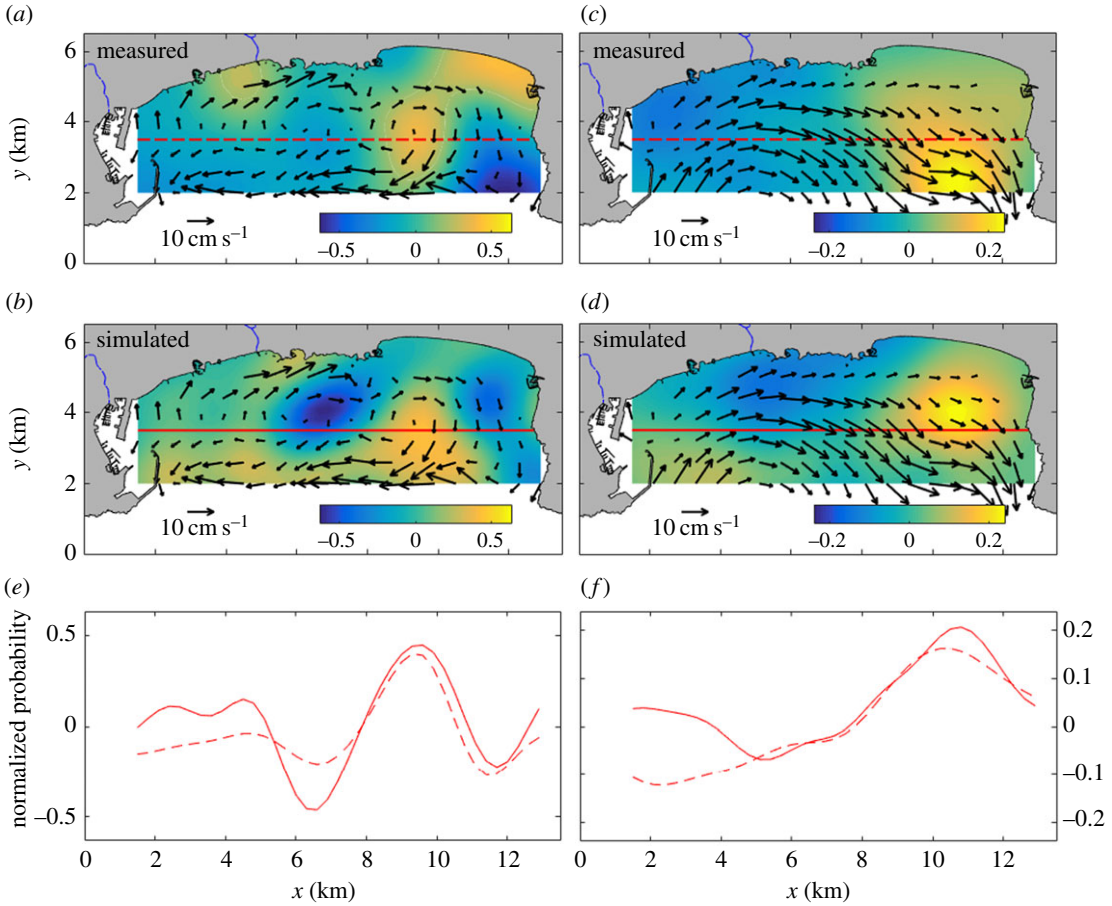


**Figure 4.** Comparison of the measured and simulated size anomalies. Near-surface distribution of (*a*) measured and (*b*) simulated preferential concentration areas (colours, dimensionless) for the June survey, and (*c*) measured and (*d*) simulated preferential concentration areas (colours, dimensionless) for the September survey. Vectors indicate near-surface ocean currents (cm $s^{-1}$) for the corresponding survey. Comparison of measured (dashed red line) and simulated (solid red line) size anomalies along the horizontal red lines in (*a–d*) for the (*e*) June and (*f*) September surveys. Blue lines over land indicate Sa Riera and Gros Torrents. (Online version in colour.)

observed at some near-shore locations of the bay. However, chlorophyll was not correlated with DIN. This suggests that the observed chlorophyll patterns were produced by phytoplankton redistribution rather than by local growth.

The highest abundances of phytoplankton were distributed in two size ranges: 11.91 ± 3.24 and 30.23 ± 5.58 µm for the June survey, and 12.28 ± 3.65 and 30.88 ± 6.29 µm for the September one. To determine these size ranges, the maxima

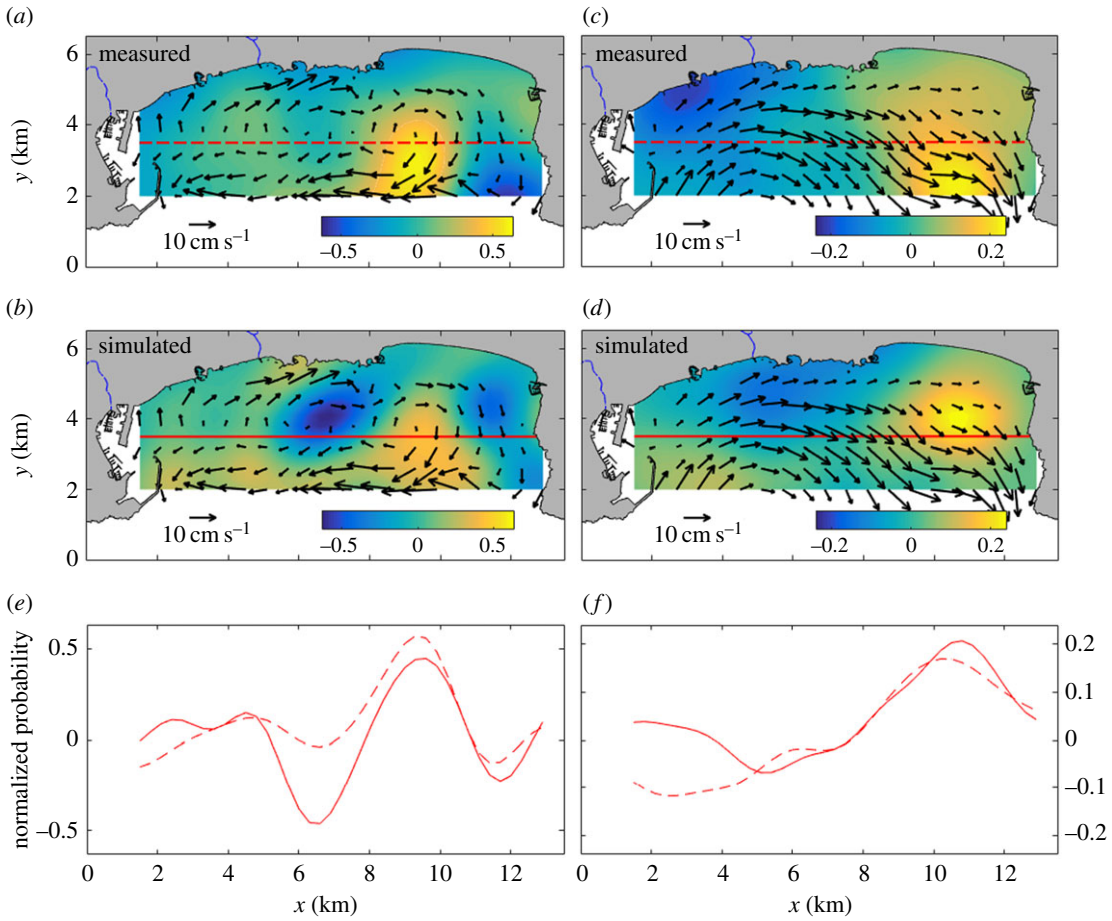


**Figure 5.** Comparison of the measured and simulated size anomalies normalized by chlorophyll. Near-surface distribution of (*a*) measured and (*b*) simulated preferential concentration areas (colours, dimensionless) for the June survey, and (*c*) measured and (*d*) simulated size anomaly areas (colours, dimensionless) for the September survey. Vectors indicate near-surface ocean for the corresponding survey. Comparison of measured (dashed red line) and simulated (solid red line) size anomalies along the horizontal red lines in (*a*–*d*) for the (*e*) June and (*f*) September surveys. Blue lines over land indicate Sa Riera and Gros Torrents. (Online version in colour.)

of phytoplankton abundance in each size class for all stations of each survey (see electronic supplementary material, figure S4) were decomposed into Gaussian peaks using an unconstrained nonlinear optimization algorithm [29]. Figure 3 shows the spatial distribution of phytoplankton in these two size ranges and the ocean currents at 5 m depth for each of the surveys. In the June survey, both phytoplankton size ranges were mainly distributed near the coast in the western side. The alongshore flow direction in this area suggests phytoplankton advection from Palma Harbour to the east. In addition, currents developed an anticyclonic gyre structure as a consequence of the strong wind event 3 days before the survey [31]. Interestingly, the large phytoplankton size range ($30.23 \pm 5.58$ µm) was almost absent inside the gyre in contrast to the small size range ($11.91 \pm 3.24$ µm). In the September survey, both phytoplankton size ranges displayed a very distinct distribution. Small size ranges ($12.28 \pm 3.65$ µm) were widely distributed in the eastern side, while large size ranges ($30.88 \pm 6.29$ µm) were localized near the coast close to Palma Harbour.

Figure 4 compares the measured size anomalies with the model results. During the June survey, measured small cells were preferentially found inside the anticyclonic gyre and near the coastal areas of the eastern side and in front of Gros Torrent. Model results were consistent with the measurements on the location of small cells inside the gyre. The agreement in the centre of the domain was very high ($r = 0.83$, $p < 0.001$), but less so in the coastal areas where DIN inputs during this survey were significant (see figure 2). Since the model only simulates advection of inertial passive cells, these discrepancies could be related to biological processes. In the September survey, small cells were preferentially found in the southeastern part of the domain. The model displayed a similar particle concentration area, although the maximum probability was slightly displaced to the north. The correlation between observed and simulated fields was also very high ($r = 0.81$, $p < 0.001$).

## 4. Discussion

In this study, we used data from two surveys and a numerical model to analyse the role of advection by ocean currents at shaping phytoplankton size structures at relatively large scales (1–10 km) in the inner part of Palma Bay (Mediterranean Sea). We explicitly took into account that phytoplankton cells have different inertial properties with respect to the surrounding fluid. Our results show significant differences in the size structure and spatial distribution of phytoplankton cells associated with the circulation patterns. The agreement between the observations and the preferential concentration model confirms that the heterogeneity in phytoplankton size structure is largely explained by the physical advection of inertial cells by the ocean currents, especially in areas relatively far from nutrient inputs.

This is the first study that provides field evidence of the relevance of inertial effects in structuring marine phytoplankton at scales greater than or equal to 1 km. The role of gyres or vortical structures in the separation of phytoplankton cells according to its size or density was previously noted by using numerical simulations [22,23] or laboratory experiments at microscales [10,40]. Smaller (or lighter) cells are concentrated in the centre of the circulation gyre, while larger (or heavier) cells are displaced outwards. This agrees fairly well with our observations in the June survey, although our spatial scales are larger. By contrast, no gyres were present in the September survey and the spatial distribution of phytoplankton was more homogeneous with smaller cells transported faster than the larger ones outside the area of study.

The model does not take into account any biological process acting on phytoplankton cells. However, discrepancies between the model and field data are mainly associated with the coastal zone of Palma Harbour. This area receives important nutrient inputs and local growth of phytoplankton as well as other processes regulating size structure, such as zooplankton grazing, may play an important role. To minimize the influence of biological processes at some coastal locations (i.e. highly productive areas), we calculated the chlorophyll-specific abundances of phytoplankton for the two main size ranges (figure 5). This reduces the relative weight of the high biomass locations with high particle abundances and, therefore, improves the correlation between field data and model results. We improve correlations from 0.15 to 0.50 for the June survey and from 0.58 to 0.82 for the September one. Likewise, correlations between model and data increase when coastal areas are excluded from the calculation (increase to 0.70 in the June survey and to 0.81 in September). This suggests that biological processes were important in these coastal areas and explains local discrepancies with the model results. Similar results are obtained when fields are normalized in terms of DIN.

Overall, our study reveals the role of inertial effects in the size distribution of phytoplankton at relatively large scales. This particle sorting mechanism may have far-reaching ecological implications for phytoplankton that range from individual to food-web interactions. Generation of spatial heterogeneity could be advantageous for phytoplankton because secondary producers with limited motion capabilities will be separated by ocean currents from the areas where phytoplankton are concentrated [10]. Further, the accumulation of cells of similar size enhances the probability of encounter between conspecific cells during sexual reproduction [41]. However, preferential concentration can be also detrimental because it increases competition for nutrients [42]. Also, some grazers have finely tuned foraging strategies that allow them to retain their position very close where phytoplankton cells are concentrated [43].

Data accessibility. Data are available from the Dryad Digital Repository at: http://dx.doi.org/10.5061/dryad.31gf4 [44].

Authors' contributions. J.S.F.-M. performed research; A.J. and G.B. designed research; I.T. and J.A. performed numerical simulations; S.A. analysed data; J.S.F.-M. wrote the first version of the paper and all authors contributed to the final version.

Competing interests. We declare we have no competing interests.

Funding. This research was partially funded by the MINECO grant GRADIENTS (CTM2012-39476-C02) and the Marie Curie International Outgoing Fellowship within the 7th European Community Framework Programme CONPLANK (PIOF-GA-2011-302562). We also acknowledge the financial support via grant FIS2013-48444-C2-1-P from the MINECO (IT). J.S.F.-M. received a Ph.D. fellowship from the Conselleria de Educació (Govern de les Illes Balears) and Fondo Social Europeo (ESF).

Acknowledgements. We are grateful to D.G. from Recursos Hidrics for river discharge data and to AEMET for meteorological data.

## References

1. Kiørboe T. 1993 Turbulence, phytoplankton cell size, and the structure of pelagic food webs. *Adv. Mar. Biol.* **29**, 1–72. (doi:10.1016/S0065-2881(08)60129-7)
2. Legendre L, Rassoulzadegan F. 1996 Food-web mediated export of biogenic carbon in oceans: hydrodynamic control. *Mar. Ecol. Prog. Ser.* **145**, 179–193. (doi:10.3354/meps145179)
3. Finkel ZV, Beardall J, Flynn KJ, Quigg A, Rees TA V, Raven JA. 2010 Phytoplankton in a changing world: cell size and elemental stoichiometry. *J. Plankton Res.* **32**, 119–137. (doi:10.1093/plankt/fbp098)
4. Li WKW, Rao S, Harrison WG, Smith JC, Cullen JJ, Irwin B, Platt T. 1983 Autotrophic picoplankton in the tropical ocean. *Science* (*Washington*) **219**, 292–295. (doi:10.1126/science.219.4582.292)
5. Azam F, Fenchel T, Field JG, Gray JS, Meyer-Reil LA, Thingstad F. 1983 The ecological role of water-column microbes in the sea. *Mar. Ecol. Prog. Ser.* **10**, 257–263. (doi:10.3354/meps010257)
6. Falkowski PG, Barber RT, Smetacek V. 1998 Biogeochemical controls and feedbacks on ocean primary production. *Science* **281**, 200–206. (doi:10.1126/science.281.5374.200)
7. Siokou-Frangou I, Christaki U, Mazzocchi MG, Montresor M, Ribera d'Alcalá M, Vaqué D, Zingone A. 2010 Plankton in the open Mediterranean Sea: a review. *Biogeosciences* **7**, 1543–1586. (doi:10.5194/bg-7-1543-2010)
8. Cushing DH. 1989 A difference in structure between ecosystems in strongly stratified waters and in those that are only weakly stratified. *J. Plankton Res.* **11**, 1–13. (doi:10.1093/plankt/11.1.1)
9. Martin AP. 2003 Phytoplankton patchiness: the role of lateral stirring and mixing. *Prog. Oceanogr.* **57**, 125–174. (doi:10.1016/S0079-6611(03)00085-5)
10. Durham WM, Climent E, Barry M, De Lillo F, Boffetta G, Cencini M, Stocker R. 2013 Turbulence drives microscale patches of motile phytoplankton. *Nat. Commun.* **4**, 2148. (doi:10.1038/ncomms3148)
11. Marquet PA, Quiñones RA, Abades S, Labra F, Tognelli M, Arim M, Rivadeneira M. 2005 Scaling and power-laws in ecological systems. *J. Exp. Biol.* **208**, 1749–1769. (doi:10.1242/jeb.01588)
12. Pasciak WJ, Gavis J. 1974 Transport limitation of nutrient uptake in phytoplankton. *Limnol. Oceanogr.* **19**, 881–888. (doi:10.4319/lo.1974.19.6.0881)
13. Taguchi S. 1976 Relationship between photosynthesis and cell size of marine diatoms. *J. Phycol.* **12**, 185–189.
14. Raven JA. 1998 The twelfth Tansley Lecture. Small is beautiful: the picophytoplankton. *Funct. Ecol.* **12**, 503–513. (doi:10.1046/j.1365-2435.1998.00233.x)
15. Marañón E. 2009 Phytoplankton size structure. In *Encyclopedia of Ocean Sciences* (eds JH Steele, KK Turekian, SA Thorpe), pp. 4252–4256. Oxford: Academic Press.
16. Kiørboe T. 2008 *A mechanistic approach to plankton ecology*. Princeton, NJ: Princeton University Press.
17. Maxey MR. 1987 The motion of small spherical particles in a cellular flow field. *Phys. Fluids* **30**, 1915–1928. (doi:10.1063/1.866206)
18. Maxey MR. 1987 The gravitational settling of aerosol particles in homogeneous turbulence and random flow fields. *J. Fluid Mech.* **174**, 441–465. (doi:10.1017/S0022112087000193)
19. Eaton JK, Fessler JR. 1994 Preferential concentration of particles by turbulence. *Int. J. Multiph. Flow* **20**, 169–209. (doi:10.1016/0301-9322(94)90072-8)

20. Squires KD, Eaton JK. 1991 Preferential concentration of particles by turbulence. *Phys. Fluids A Fluid Dyn*. **3**, 1169–1178. (doi:10.1063/1.858045)
21. Reigada R, Sagués F, Sancho JM. 2001 Inertial effects on reactive particles advected by turbulence. *Phys. Rev. E. Stat. Nonlin. Soft Matter Phys*. **64**, 26307. (doi:10.1103/PhysRevE.64.026307)
22. Squires KD, Yamazaki H. 1995 Preferential concentration of marine particles in isotropic turbulence. *Deep Sea Res. Part I Oceanogr. Res. Pap*. **42**, 1989–2004. (doi:10.1016/0967-0637(95)00079-8)
23. Reigada R, Hillary RM, Bees MA, Sancho JM, Sagues F. 2003 Plankton blooms induced by turbulent flows. *Proc. R. Soc. Lond. B* **270**, 875–880. (doi:10.1098/rspb.2002.2298)
24. Cartwright JHE, Magnasco MO, Piro O, Tuval I. 2002 Bailout embeddings and neutrally buoyant particles in three-dimensional flows. *Phys. Rev. Lett*. **89**, 264501. (doi:10.1103/PhysRevLett.89.264501)
25. Massutí E *et al.* 2008 The influence of oceanographic scenarios on the population dynamics of demersal resources in the western Mediterranean: hypothesis for hake and red shrimp off Balearic Islands. *J. Mar. Syst*. **71**, 421–438. (doi:10.1016/j.jmarsys.2007.01.009)
26. Jordi A, Basterretxea G, Anglès S. 2009 Influence of ocean circulation on phytoplankton biomass distribution in the Balearic Sea: study based on sea-viewing wide field-of-view sensor and altimetry satellite data. *J. Geophys. Res. Oceans* **114**, C11005. (doi:10.1029/2009JC005301)
27. Basterretxea G, Jordi A, Garcés E, Anglès S, Reñé A. 2011 Seiches stimulate transient biogeochemical changes in a microtidal coastal ecosystem. *Mar. Ecol. Prog. Ser*. **423**, 15–28. (doi:10.3354/meps08949)
28. Tovar-Sánchez A, Basterretxea G, Rodellas V, Sánchez-Quiles D, García-Orellana J, Masqué P, Jordi A, López JM, Garcia-Solsona E. 2014 Contribution of groundwater discharge to the coastal dissolved nutrients and trace metal concentrations in Majorca Island: karstic vs detrital systems. *Environ. Sci. Technol*. **48**, 11 819–11 827. (doi:10.1021/es502958t)
29. Font-Muñoz JS, Jordi A, Angles S, Basterretxea G. 2015 Estimation of phytoplankton size structure in coastal waters using simultaneous laser diffraction and fluorescence measurements. *J. Plankton Res*. **37**, 740–751. (doi:10.1093/plankt/fbv041)
30. Jordi A, Basterretxea G, Wang DP. 2009 Evidence of sediment resuspension by island trapped waves. *Geophys. Res. Lett*. **36**, L18610. (doi:10.1029/2009GL040055)
31. Jordi A, Basterretxea G, Wang D-P. 2011 Local versus remote wind effects on the coastal circulation of a microtidal bay in the Mediterranean Sea. *J. Mar. Syst*. **88**, 312–322. (doi:10.1016/j.jmarsys.2011.05.007)
32. Jordi A, Wang D-P. 2013 Estimation of transport at open boundaries with an ensemble Kalman filter in a coastal ocean model. *Ocean Model*. **64**, 56–66. (doi:10.1016/j.ocemod.2013.01.002)
33. Grasshoff K, Ehrhardt M, Kremling K. 1983 *Methods of seawater analysis*. Weinheim/Deerfield Beach, FL: Verlag Chemie.
34. Gandin LS. 1963 Objective analysis of meteorological fields. *Gidrometeorol. Izd*. **92**, 242.
35. Maxey MR, Riley JJ. 1983 Equation of motion for a small rigid sphere in a nonuniform flow. *Phys. Fluids* **26**, 883–889. (doi:10.1063/1.864230)
36. Tio K-K, Liñán A, Lasheras JC, Gañán-Calvo AM. 1993 On the dynamics of buoyant and heavy particles in a periodic Stuart vortex flow. *J. Fluid Mech*. **254**, 671. (doi:10.1017/S0022112093002307)
37. Arrieta J, Barreira A, Tuval I. 2015 Microscale patches of nonmotile phytoplankton. *Phys. Rev. Lett*. **114**, 128102. (doi:10.1103/PhysRevLett.114.128102)
38. Ramis C, Jansá A, Alonso S. 1990 Sea breeze in Mallorca. A numerical study. *Meteorol. Atmos. Phys*. **42**, 249–258. (doi:10.1007/BF01314828)
39. Rodellas V, Garcia-Orellana J, Tovar-Sánchez A, Basterretxea G, López-Garcia JM, Sánchez-Quiles D, Garcia-Solsona E, Masqué P. 2014 Submarine groundwater discharge as a source of nutrients and trace metals in a Mediterranean bay (Palma Beach, Balearic Islands). *Mar. Chem*. **160**, 56–66. (doi:10.1016/j.marchem.2014.01.007)
40. De Lillo F, Cencini M, Durham WM, Barry M, Stocker R, Climent E, Boffetta G. 2014 Turbulent fluid acceleration generates clusters of gyrotactic microorganisms. *Phys. Rev. Lett*. **112**, 44502. (doi:10.1103/PhysRevLett.112.044502)
41. Waite A, Harrison PJ. 1992 Role of sinking and ascent during sexual reproduction in the marine diatom *Ditylutn hrightwellii*. *Mar. Ecol. Prog. Ser*. **87**, 113–122. (doi:10.3354/meps087113)
42. Siegel DA. 1998 Resource competition in a discrete environment: why are plankton distributions paradoxical? *Limnol. Oceanogr*. **43**, 1133–1146. (doi:10.4319/lo.1998.43.6.1133)
43. Tiselius P, Jonsson PR, Verity PG. 1993 A model evaluation of the impact of food patchiness on foraging strategy and predation risk in zooplankton. *Bull. Mar. Sci*. **53**, 247–264.
44. Font-Muñoz JS, Jordi A, Tuval I, Arrieta J, Anglès S, Basterretxea G. 2017 Data from: Advection by ocean currents modifies phytoplankton size structure. Dryad Digital Repository. (http://dx.doi.org/10.5061/dryad.31gf4)